

## Measurement of Deoxyribose $^3J_{\text{HH}}$ Scalar Couplings Reveals Protein Binding-Induced Changes in the Sugar Puckers of the DNA

Thomas Szyperski,<sup>†</sup> César Fernández,<sup>†</sup> Akira Ono,<sup>‡</sup> Masatsune Kainosho,<sup>\*‡</sup> and Kurt Wüthrich<sup>\*‡</sup>

Institut für Molekularbiologie und Biophysik  
Eidgenössische Technische Hochschule-Hönggerberg  
CH-8093 Zürich, Switzerland  
Department of Chemistry, Faculty of Science  
Tokyo Metropolitan University,  
1-1 Minamiohsawa, Hachioji 192-03, Japan

Received September 2, 1997

Revised Manuscript Received November 24, 1997

$^3J_{\text{HH}}$  scalar couplings are most useful to assess the sugar pucker in NMR structure determinations of DNA duplexes.<sup>2,3</sup> Such couplings can be obtained from 2D  $^1\text{H}$ – $^1\text{H}$  COSY,<sup>3,4</sup> but spectral overlap and mutual cancellation limit this approach to smaller systems. Above approximately 5 kDa, scalar couplings can be extracted from  $^{13}\text{C}$ -resolved spectra of  $^{13}\text{C}$ -labeled nucleic acids.<sup>5–7</sup> In this paper, we show that 3D  $^{13}\text{C}$ -resolved in-phase [ $^1\text{H}$ ,  $^1\text{H}$ ]-COSY (3D HCH-COSY)<sup>8</sup> is a powerful experiment to derive values for  $^3J_{1'2'}$ ,  $^3J_{1'2''}$ ,  $^3J_{2'3'}$ ,  $^3J_{2'3''}$ , and  $^3J_{3'4'}$  in DNA, which yield constraints<sup>10</sup> for the deoxyribose dihedral angles<sup>9</sup>  $\nu_1$ ,  $\nu_2$ , and  $\nu_3$ . The couplings were determined for a uniformly  $^{13}\text{C}/^{15}\text{N}$ -labeled 14-base pair DNA duplex prepared by solid-phase synthesis,<sup>11</sup> which binds to the *Antp(C39S)* homeodomain<sup>12</sup> to form a 17 kDa protein–DNA complex.<sup>13</sup>

3D HCH-COSY is a quantitative  $J$  correlation experiment<sup>14</sup> that yields  $^3J_{\text{HH}}$  from intensity ratios of  $^{13}\text{C}$ -resolved  $^1\text{H}$ – $^1\text{H}$  diagonal peaks and cross peaks.<sup>8</sup> Here, the experiment has been adapted for  $^{13}\text{C}$ -labeled nucleic acids. The large spectral dispersion encountered for  $^{13}\text{C}$ -labeled DNA favors the extraction of a large number of couplings. Measurements of  $^3J_{1'2'}$  and  $^3J_{1'2''}$

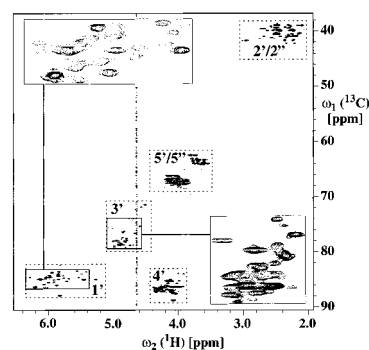


**Figure 1.** Spectral regions containing deoxyribose resonances from 2D *ct*- $^{13}\text{C}$ ,  $^1\text{H}$ -COSY<sup>17</sup> and 3D HCH-COSY spectra<sup>8</sup> of a uniformly  $^{13}\text{C}$ ,  $^{15}\text{N}$ -labeled DNA duplex in a complex with the *Antp(C39S)* homeodomain (concentration 1 mM,  $T = 36$  °C, pH = 6.0). The dotted rectangles identify spectral regions of specified proton types. The two solid rectangles identify the regions of the 2D spectrum for which the corresponding spectral regions taken from a projection along  $\omega_2(^1\text{H})$  of the 3D spectrum are shown in the inserts. Chemical shifts are relative to internal DSS. The 3D HCH-COSY spectrum was recorded on a Bruker AMX500 spectrometer equipped with a  $^1\text{H}$ - $\{^{13}\text{C}, ^{31}\text{P}\}$  triple-resonance probehead. The setup was as in ref 8, except that the parameters  $T^1 = 4.631$  ms and  $T^{\text{H}} = 7.853$  ms were adapted to the deoxyribose carbon–carbon one-bond scalar couplings, thus yielding  $\delta = 7.720$  ms and  $\delta' = 7.837$  ms (see Figure 1 in ref 8).  $^{31}\text{P}$  was decoupled with a WALTZ16 sequence<sup>25</sup> during the presence of transverse  $^{13}\text{C}$ -magnetization;  $84(t_1) \times 55(t_2) \times 256(t_3)$  complex points were accumulated in  $\sim 3.5$  days, with  $t_{1,\text{max}}(^{13}\text{C}) = 20.0$  ms,  $t_{2,\text{max}}(^1\text{H}) = 13.6$  ms, and  $t_{3,\text{max}}(^1\text{H}) = 63.9$  ms. Prior to Fourier transformation, the data matrix was extended by linear prediction by 60 complex points along  $t_1$ , and 40 complex points along  $t_2$ . The 2D *ct*- $^{13}\text{C}$ ,  $^1\text{H}$ -COSY spectrum was recorded on a Varian Unity750+ spectrometer equipped with a  $^1\text{H}$ - $\{^{13}\text{C}, ^{15}\text{N}\}$  triple-resonance probehead, using a constant-time delay of 23 ms;  $245(t_1) \times 512(t_2)$  complex points were accumulated in 2.4 h, with  $t_{1,\text{max}}(^{13}\text{C}) = 22.8$  ms and  $t_{2,\text{max}}(^1\text{H}) = 55.5$  ms.

<sup>†</sup> Eidgenössische Technische Hochschule-Hönggerberg.

<sup>‡</sup> Tokyo Metropolitan University.

(1) Abbreviations used: NMR, nuclear magnetic resonance; 2D, two-dimensional; 3D, three-dimensional; *ct*, constant-time; COSY, correlation spectroscopy; 3D HCH–COSY, 3D  $^{13}\text{C}$ -resolved in-phase [ $^1\text{H}$ ,  $^1\text{H}$ ]-COSY;  $^3J_{\text{XY}}$ , vicinal scalar coupling between protons X and Y; DNA, deoxyribonucleic acid; *Antp*, *Antennapedia*; HD, homeodomain; *Antp(C39S)*, mutant 68-residue *Antp* homeodomain polypeptide with the homeodomain sequence in positions 1 to 60 and Cys39 replaced by Ser; DSS, 2,2-dimethyl-2-silapentane-5-sulfonic acid.

(2) Wüthrich, K. *NMR of Proteins and Nucleic Acids*; Wiley: New York, 1986.

(3) (a) Rinkel, L. J.; Altona, C. J. *Biomol. Struct. Dyn.* **1987**, *4*, 621–649. (b) Celda, B.; Widmer, H.; Leupin, W.; Chazin, W. J.; Denny, W. A.; Wüthrich, K. *Biochemistry* **1989**, *28*, 1462–1471. (c) Majumdar, A.; Hosur, R. V. *Prog. NMR Spectrosc.* **1992**, *24*, 109–158. (d) Wijmenga, S. S.; Mooren, M. M. W.; Hilbers, C. W. in *NMR of Macromolecules*; Roberts, G. C. K., Ed.; Oxford University Press: Oxford, 1993; pp 217–288.

(4) (a) Rance, M.; Sørensen, O. W.; Bodenhausen, G.; Wagner, G.; Ernst, R. R.; Wüthrich, K. *Biochem. Biophys. Res. Commun.* **1983**, *117*, 479–485. (b) Griesinger, C.; Sørensen, O. W.; Ernst, R. R. *J. Am. Chem. Soc.* **1985**, *107*, 6394–6396. (c) Widmer, H.; Wüthrich, K. *J. Magn. Reson.* **1987**, *74*, 316–336.

(5) (a) Eggenberger, U.; Karimi-Nejad, Y.; Thüning, H.; Rüterjans, H.; Griesinger, C. *J. Biomol. NMR* **1992**, *2*, 583–590. (b) Schwalbe, H.; Marino, J. P.; Glaser, S. J.; Griesinger, C. *J. Am. Chem. Soc.* **1995**, *117*, 7251–7252.

(6) Varani, G.; Aboul-ela, F.; Allain, F. H.-T. *Prog. NMR Spectrosc.* **1996**, *29*, 51–127.

(7) Ono, A.; Tate, S.; Ishido, Y. A.; Kainosho, M. *J. Biomol. NMR* **1994**, *4*, 581–586.

(8) Grzesiek, S.; Kuboniwa, H.; Hinck, A. P.; Bax, A. *J. Am. Chem. Soc.* **1995**, *117*, 5312–5315.

(9) Saenger, W. *Principles of Nucleic Acid Structure*; Springer: New York, 1984.

(10) Haasnoot, C. A. G.; DeLeuw, F. A. A. M.; Altona, C. *Tetrahedron* **1980**, *36*, 2783–2792.

(11) See ref 8 in the following: Szyperski, T.; Ono, A.; Fernández, C.; Iwai, H.; Tate, S.; Wüthrich, K.; Kainosho, M. *J. Am. Chem. Soc.* **1997**, *119*, 9901–9902.

(12) Müller, M.; Affolter, M.; Leupin, W.; Otting, G.; Wüthrich, K.; Gehring, W. J. *EMBO J.* **1988**, *7*, 4299–4304.

benefit from the large dispersion of C1'–H1' cross peaks, and measurements of  $^3J_{2'3'}$ ,  $^3J_{2'3''}$ , and  $^3J_{3'4'}$  benefit from the good separation of C3'–H3' signals (Figure 1). This enables integration of most diagonal peaks  $\{\omega_1(\text{C1}'), \omega_2(\text{H1}'), \omega_3(\text{H1}')\}$  and  $\{\omega_1(\text{C3}'), \omega_2(\text{H3}'), \omega_3(\text{H3}')\}$ , which is essential for obtaining the couplings. These diagonal peaks are separated from the cross peaks with H2' and H2'' chemical shifts along  $\omega_2$  (Figures 1 and 2). The separation of H3' and H4' resonances suffices to resolve most diagonal peaks  $\{\omega_1(\text{C3}'), \omega_2(\text{H3}'), \omega_3(\text{H3}')\}$  and the corresponding cross peaks that involve H4' along  $\omega_2$ , which enables the determination of  $^3J_{3'4'}$  (Figures 1 and 3).

For accurate determination of  $^3J_{\text{HH}}$ , one needs to consider that rapid  $^1\text{H}$ – $^1\text{H}$  spin flips lead to faster relaxation of antiphase magnetization when compared with in-phase magnetization.<sup>8,15,16</sup> We measured the relaxation times of the two-spin order  $H_z C_z$ ,  $T_{1zz}$ , from two 2D *ct*- $^{13}\text{C}$ ,  $^1\text{H}$ -COSY experiments<sup>17</sup> (recording times: 4 h for the free and 16 h for the complexed DNA) in which  $H_z C_z$  was stored for delays of either  $\tau_1 = 1$  ms or  $\tau_2 = 31.1$  ms after the first INEPT. Since  $T_1(^{13}\text{C}) \gg T_{1zz}$ , the intensity ratio  $I_1(\tau_1)/I_2(\tau_2)$  provides an estimate for the apparent selective  $T_1$  relaxation times of the protons.<sup>16</sup> For the free DNA, we obtained  $T_{1,\text{sel}}(\text{H2}'/\text{H2}'') = 160 \pm 10$  ms and  $T_{1,\text{sel}}(\text{H4}') = 165 \pm 10$  ms for the nonterminal nucleotides. Hence, couplings derived via generation of magnetization that is antiphase with respect to H2'/H2'' or H4'

(13) Billeter, M.; Qian, Y. Q.; Otting, G.; Müller, M.; Gehring, W.; Wüthrich, K. *J. Mol. Biol.* **1993**, *234*, 1084–1097.

(14) Bax, A.; Vuister, G. W.; Grzesiek, S.; Delaglio, F.; Wang, A. C.; Tschudin, R.; Zhu, G. *Methods Enzymol.* **1993**, *239*, 79–105.

(15) Harbison, G. J. *J. Am. Chem. Soc.* **1993**, *115*, 3026–3027.

(16) Vuister, G. W.; Bax, A. *J. Am. Chem. Soc.* **1993**, *115*, 7772–7777.

(17) (a) Santoro, J.; King, G. C. *J. Magn. Reson.* **1992**, *97*, 202–207. (b) Vuister, G. W.; Bax, A. *J. Magn. Reson.* **1992**, *98*, 428–435.

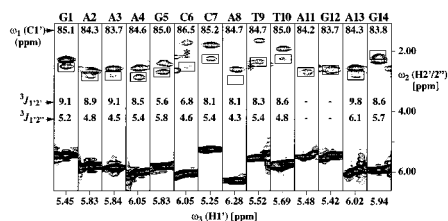


**Figure 2.** Contour plots of  $[\omega_2(^1\text{H})]$ ,  $[\omega_3(^1\text{H})]$  strips taken at the  $^{13}\text{C}1'$  chemical shifts (indicated at the top of the strips) from a 500 MHz 3D HCH-COSY spectrum<sup>8</sup> (see Figure 1) of the *Antp*(C39S) homeodomain-DNA complex. Along  $\omega_3$ , the strips are centered about the H1' chemical shifts. Except for G<sub>14</sub>, the upper field and lower field cross peaks encode the H2' and H2'' chemical shifts, respectively. The H2'' cross peaks are shown in boxes. The strips belong to the DNA strand with the nucleotide sequence indicated at the top. The diagonal peaks and the cross peaks have opposite sign.<sup>8</sup> Cross peaks belonging to spin systems of the other DNA strand are marked with an asterisk. Chemical shifts are relative to internal DSS.  $^3J_{1'2'}$  and  $^3J_{1'2''}$  values are given below the cross peaks (no data are given for A<sub>11</sub> and G<sub>12</sub> because the chemical shifts differences between H2' and H2'' are smaller than 0.1 ppm). To assess the experimental error, we performed the 3D HCH-COSY experiment twice. The average pairwise difference between the scalar couplings extracted from the two spectra was 0.4 Hz. Assuming a correction factor of  $1.15 \pm 0.05$  to account for relaxation effects, we obtain, according to the Gaussian law of error propagation, an uncertainty between  $\pm 0.5$  and  $\pm 0.7$  Hz for couplings ranging from 2 to 9 Hz.

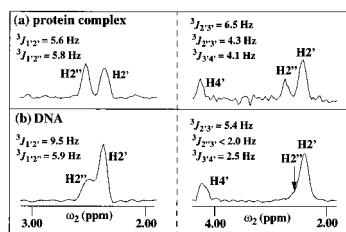


**Figure 3.** One-dimensional cross sections along  $\omega_2(^1\text{H})$  taken from 3D HCH-COSY spectra. (a) Same 500 MHz spectrum of the *Antp*(C39S) homeodomain-DNA complex as shown in Figures 1 and 2. (b) Recorded for a 1 mM solution of the free DNA duplex ( $T = 36^\circ\text{C}$ ,  $\text{pH} = 6.0$ , 50 mM  $\text{KPO}_4$ , 20 mM  $\text{Cl}$ ). The cross sections on the left were taken at  $\omega_1(^{13}\text{C}1')/\omega_3(^{13}\text{H}1')$  of G<sub>5</sub>, and the cross sections on the right at  $\omega_1(^{13}\text{C}3')/\omega_3(^{13}\text{H}3')$  of the same nucleotide.  $^3J_{\text{HH}}$  values derived from these data are indicated. The change of the couplings upon protein binding is apparent from the change in relative cross peak intensities. For the free duplex, the spectrum was recorded on a Bruker DRX600 spectrometer equipped with a  $^1\text{H}$ - $^{13}\text{C}$ ,  $^{15}\text{N}$  triple-resonance probehead and processed as described in Figure 1, except that no  $^{31}\text{P}$ -decoupling was applied;  $87(t_1) \times 55(t_2) \times 256(t_3)$  complex points were accumulated in 22 h, with  $t_{1,\text{max}}(^{13}\text{C}) = 20.7$  ms,  $t_{2,\text{max}}(^1\text{H}) = 13.6$  ms and  $t_{3,\text{max}}(^1\text{H}) = 63.9$  ms.

are only about 3% smaller than the true couplings (see Figure 3 in ref 16). For the *Antp*(C39S) homeodomain-DNA complex, we obtained  $T_{1,\text{sel}}(\text{H}2'/\text{H}2'') = 100 \pm 15$  ms and  $T_{1,\text{sel}}(\text{H}4') = 110 \pm 20$  ms, indicating a correction of about 8%.<sup>18</sup> For protons of a methylene group (H2' and H2'') both coupled to a third proton (H1' or H3'), spin flips between the methylene protons occurring during the dephasing period  $2\delta$  decrease the value measured for the larger coupling and increase the value for the smaller one.<sup>19</sup> This effect scales with the difference between the two couplings, which is generally smaller than about 5 Hz for deoxyribose rings.<sup>3</sup> Hence, such a correction is often not required. From  $^1\text{H}$ - $^1\text{H}$  NOESY spectra, the cross relaxation rates  $\sigma_{2'2''}$  could be estimated to be about  $4\text{ s}^{-1}$  for the free DNA and about  $10\text{ s}^{-1}$  for the complex, respectively. We thus corrected only pairs of couplings in the complex which differed by more than 3 Hz (0.2 Hz was

then subtracted from the smaller and added to the larger coupling).<sup>20</sup> Spin flips between H2' and H2'' that occur during the rephasing period diminish the amount of magnetization refocused after a delay  $2\delta'$  by  $\int_0^{2\delta'} \cos(\pi^3 J t) e^{-\sigma_{2'2''} t} dt / (\int_0^{2\delta'} \cos(\pi^3 J t) dt)$ . Hence, except for  $^3J_{3'4'}$ , couplings ranging from 2 to 9 Hz have to be corrected further by 4–7% for the complex, and by 0–3% for the free DNA.

For the free DNA, 135 out of 136  $^3J_{\text{HH}}$  values (99%) involving nondegenerate H2' and H2'' chemical shifts were determined (27  $^3J_{1'2'}$ , 26  $^3J_{1'2''}$ , 27  $^3J_{2'3'}$ , 27  $^3J_{2'3''}$ , and 28  $^3J_{3'4'}$ ). For the complex, 97 out of 128  $^3J_{\text{HH}}$  values (76%) were measured (22  $^3J_{1'2'}$ , 21  $^3J_{1'2''}$ , 16  $^3J_{2'3'}$ , 16  $^3J_{2'3''}$ , and 22  $^3J_{3'4'}$ ). The large number of couplings provides a sound basis for analysis of the deoxyribose conformations in free DNA and the protein-DNA complex.<sup>3</sup> This allows, for the first time, investigation of conformational changes of the sugar rings upon complexation with a protein in solution: Figure 3 provides evidence for a conformational shift induced at G<sub>5</sub>, which exhibits numerous contacts with the protein.<sup>13</sup> Interpretation in the framework of a two-state model<sup>21</sup> assuming rapid interconversion of the C2'-endo and C3'-endo forms (pucker amplitude  $35^\circ$ ) yields 85–95% and 45–70% C2'-endo conformer for the free DNA and the complex, respectively.<sup>22</sup>

The analysis of the sugar rings is of particular interest for B-type DNA. Although centered around C2'-endo, the deoxyribose conformations are broadly distributed from C3'-exo to O4'-endo, which contrasts with the much tighter clustering around C3'-endo in A-type helices.<sup>21,23</sup> Since this conformational polymorphism could play a role for sequence-specific protein-DNA recognition, use of the presently proposed approach for high-quality NMR structure determinations of DNA and their protein complexes is of interest. In X-ray structures, the determination of the sugar pucker is usually warranted only at a resolution of 2.0 Å or better.<sup>21</sup> Currently, there are only two X-ray structures of protein-DNA complexes in the Brookhaven Protein Databank for which the deoxyribose conformations were determined.<sup>24</sup> Hence, unique structural information about DNA conformation in protein complexes can be obtained by NMR that is not readily accessible from X-ray diffraction data.

**Acknowledgment.** Financial support was obtained from the Schweizerischer Nationalfonds (project 31-49047.96), from the ETH Zürich for a special grant within the framework of the Swiss/Japanese R & D Roundtable Collaboration, and by CREST (Core Research for Evolutional Science and Technology) of the Japan Science and Technology Corporation (JST).

JA9730551

(20) To estimate this correction, we consider a three-spin system consisting of proton A and the geminal protons K and L, where A and K, and A and L exhibit three-bond scalar couplings  $J_1$  and  $J_2$ , respectively, with  $J_1 > J_2$ . A, K, and L denote the corresponding spin operators. The magnetization transfer  $2A_x K_z \rightarrow 2A_x L_z$  mediated by K-L spin flips during  $2\delta$  is small compared with the generation of  $2A_x K_z$  and  $2A_x L_z$  coherence due to  $J_1$  and  $J_2$ , and may thus be approximated by  $d/dt[2A_x K_z(t)] = -\sigma_{\text{KL}}\{[2A_x K_z(t)] - [2A_x L_z(t)]\} = -\sigma_{\text{KL}}(\sin \pi J_1 t - \sin \pi J_2 t)$ , where  $\sigma_{\text{KL}}$  is the cross-relaxation rate between K and L. Integration from  $t = 0$  to  $t = 2\delta$  with  $\sin \pi J t \approx \pi J t$  yields  $\Delta[2A_x K_z] = -2\pi\delta^2 \sigma_{\text{KL}}(J_1 - J_2)$ , where  $\Delta[2A_x K_z]$  represents the amount of antiphase magnetization transformed from  $2A_x K_z$  into  $2A_x L_z$  at  $t = 2\delta$ . The apparent scalar couplings,  $J_1^{\text{app}}$  and  $J_2^{\text{app}}$ , are then given by

$$J_i^{\text{app}} = (1/2\pi\delta) \arctan \left\{ \sqrt{[(\sin \pi J_1 2\delta / \cos J_2 2\delta)^2 - \sigma_{\text{KL}} \delta (J_1 - J_2) / J_1]} \right\}$$

with  $i = 1, 2$ . Setting  $J_1$  and  $J_2$  to the experimental values, the difference between experimental and calculated apparent coupling provides a good estimate for the correction.

(21) Hartmann, B.; Lavery, R. *Quart. Rev. Biophys.* **1996**, *29*, 309–368.

(22) Assuming a single deoxyribose conformation,  $^3J_{1'2'}$  indicates a transition from C2'-endo to O4'-endo. However, the remaining couplings are not consistent with an O4'-endo conformation, which strongly suggests that an equilibrium between at least two states has to be invoked. This view is supported by  $^{13}\text{C}$ -resolved  $^1\text{H}$ - $^1\text{H}$  NOESY: the H1'-H4' NOE observed for G<sub>5</sub> in the complex is not stronger than those of the other nucleotides in the complex, whereas a stronger H1'-H4' NOE is expected for O4'-endo.<sup>2</sup>

(23) Privé, G. G.; Yanagi, K.; Dickerson, R. E. *J. Mol. Biol.* **1991**, *217*, 177–199.

(24) (a) Lahm, A.; Suck, D. *J. Mol. Biol.* **1991**, *221*, 645–667. (b) Kim, J. L.; Burley, S. K. *Nat. Struct. Biol.* **1994**, *9*, 638–653.

(25) Shaka, A. J.; Lee, C. J.; Pines, A. J. *J. Magn. Reson.* **1983**, *52*, 335–338.

(18) For the present systems, the same corrections can be applied for scalar couplings derived from the generation of antiphase magnetization with respect to either H1', H3', or H5'/H5'' protons. The  $T_{1,\text{sel}}(^1\text{H})$  values are: Free DNA H1', 240  $\pm$  20 ms; H3', 200  $\pm$  10 ms; H5'/H5'', 180  $\pm$  20 ms. Complex H1', 120  $\pm$  20 ms; H3', 100  $\pm$  20 ms; H5'/H5'', 110  $\pm$  20 ms.

(19) Vuister, G. W.; Yamazaki, T.; Torchia, D. A.; Bax, A. *J. Biomol. NMR.* **1993**, *3*, 297–306.